Discrete interactions in cell adhesion measured by single-molecule force spectroscopy

Martin Benoit*†, Daniela Gabriel‡, Günther Gerisch‡ and Hermann E. Gaub*

*Centre for Nanoscience, Ludwig Maximilians Universität München, Amalienstraβe 54, D-80799 München, Germany
‡Max Planck Institut für Biochemie, Am Klopferspitz 18a, D-82152 Martinsried, Germany
†e-mail: Martin.Benoit@physik.uni-muenchen.de

Cell–cell adhesion mediated by specific cell-surface molecules is essential for multicellular development. Here we quantify de-adhesion forces at the resolution of individual cell-adhesion molecules, by controlling the interactions between single cells and combining single-molecule force spectroscopy with genetic manipulation. Our measurements are focused on a glycoprotein, contact site A (csA), as a prototype of cell-adhesion proteins. csA is expressed in aggregating cells of *Dictyostelium discoideum*, which are engaged in development of a multicellular organism. Adhesion between two adjacent cell surfaces involves discrete interactions characterized by an unbinding force of 23 ±8 pN, measured at a rupture rate of 2.5±0.5 μm s^{-1}.

Cell-adhesion molecules regulate essential processes in multicellular organisms such as embryonic development, neuronal pathfinding and the binding of white blood cells to the walls of blood vessels[1–3]. Cells may carry several different adhesion molecules[4], resulting in a large variation in the molecular repertoires of cell surfaces. This variability is reflected by the complicated pattern of signal transduction, cell motility and other adhesion-controlled cellular functions during animal development and adult life.

We aimed to develop an experimental platform to investigate cell–cell interactions *in vivo* at the single-molecule level. For this purpose, cells of the eukaryote *D. discoideum* offer the advantage that one particular type of adhesion molecule, the developmentally regulated csA glycoprotein, can be singled out by genetic manipulation[5]. In *D. discoideum*, csA participates in cell aggregation, the transition from single cells to the multicellular stage[6]. The cell-adhesion system of aggregating cells involves membrane–membrane recognition and discriminates between self and non-self. As a result of this specificity, cells of different species are able to sort themselves from a mixture[7,8].

The *csA* gene is expressed under the control of cyclic-AMP signals that precede the aggregation stage of multicellular development. Thus, csA is undetectable in growth-phase cells, but is expressed upon starvation[9]. In developing cells at the aggregation stage, csA covers roughly 2% of the total cell-surface area, a finding that supports the idea that adhesive interactions occur at specific sites on the cell surface[10]. CsA molecules react with each other, forming non-covalent bonds that link the surfaces of adjacent cells[11]. CsA is anchored in the plasma membrane by a ceramide-based phospholipid[12]. This lipid anchor, which guarantees a long residence time of csA on the cell surface, can be replaced by a polypeptide transmembrane domain without loss of cell adhesion[13].

Adhesion between individual cells, such as granulocytes and target cells, has previously been measured using mechanical methods, such as micropipette manipulation[14,15] and induction of hydrodynamic stress[16,17]. Scanning force microscopy (SFM)[18] has facilitated the development of piconewton-scale instrumentation, which provides force resolution and positional precision that allows measurements at the single-molecule level[19,20]. Forces for conformational transitions in polysaccharides[21,22], for protein unfolding[23–25] and for stretching and unzipping of DNA[26,27] have been measured. Unbinding forces for individual receptor–ligand pairs have also been determined[28–31], and basic features of their binding potentials reconstructed[32,33]. Here we apply single-molecule force spectroscopy to the analysis of cell adhesion in living cells.

Results

Measurement of adhesion forces between individual cells. Using the light microscope of a custom-made force spectrometer for guid-

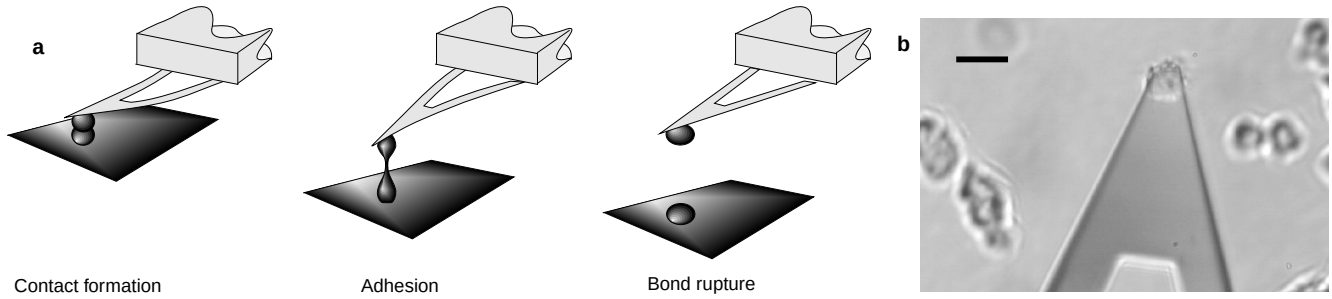

Figure 1 **Force spectroscopy of adhesion between individual *D. discoideum* cells. a**, Principal features of the experimental procedure (see Methods). Forces required for bond rupture were measured. **b**, Light-microscopic image of a cantilever-mounted cell before being brought into contact with another cell. Scale bar represents 20 μm.

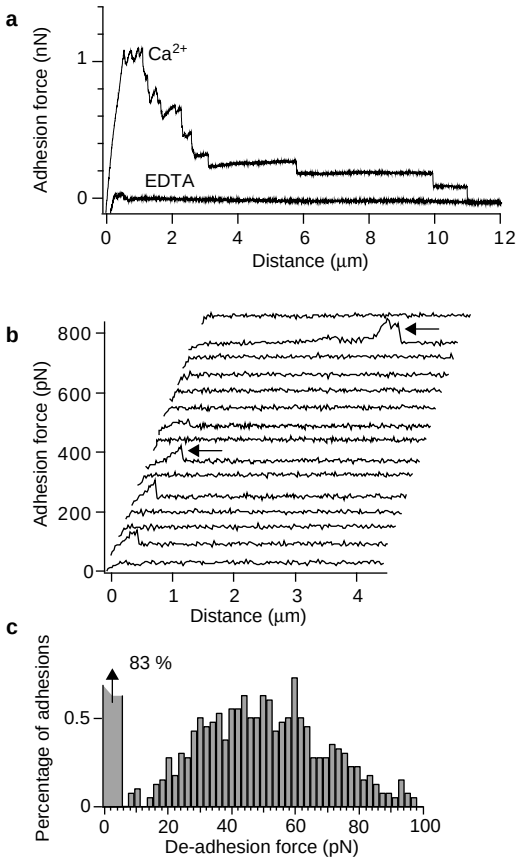

Figure 2 **Force spectra for Ca^{2+}-dependent adhesion between cells in the growth phase. a**, Force-spectroscopy traces for *D. discoideum* cells. Cell–cell contacts were maintained for 20 s at 150±20 pN and the cells subsequently pulled apart at a speed of 1.5 μm s^{-1}. Note the strong de-adhesion forces and stepwise separation of cells in the Ca^{2+} trace. In the undeveloped cells used here, cell–cell adhesion depends on the presence of Ca^{2+}. Upon removal of Ca^{2+} by EDTA, adhesion forces are markedly reduced (EDTA trace). **b**, Force-spectroscopy traces for cell–cell contacts maintained for 0.2 s at 35±5 pN. Note that de-adhesion occurred predominantly in single steps. Arrows indicate force steps for complete rupture as shown in **c**. **c**, Histogram of de-adhesion forces for 5,760 traces. Note the broad peak at about 50 pN. Rupture events occurring at <7 pN are represented by the first bar.

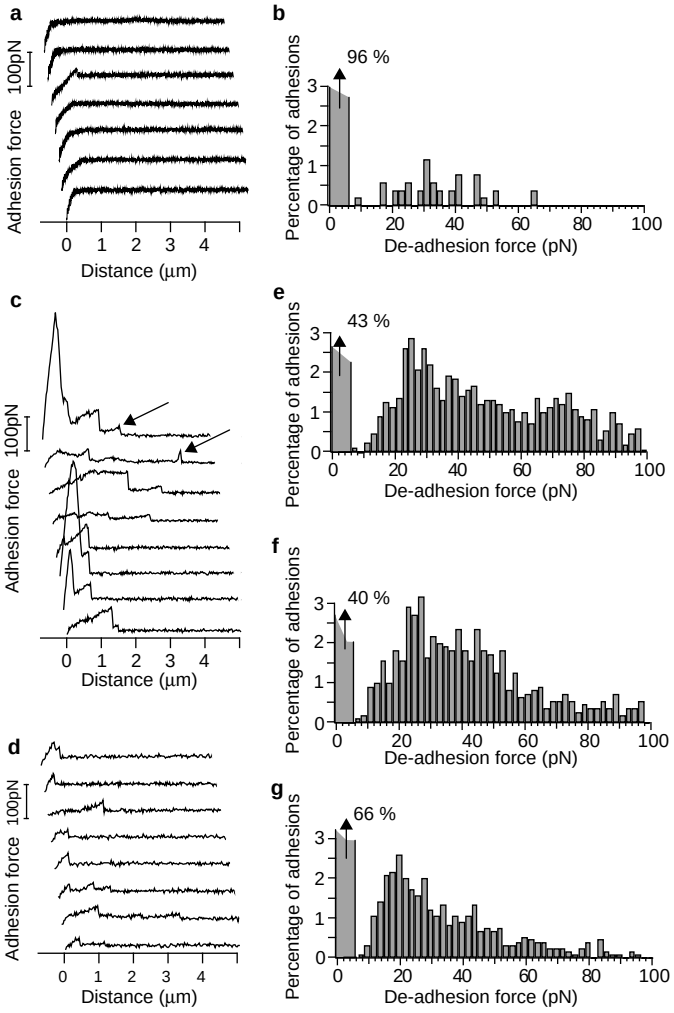

Figure 3 **Force spectra for EDTA-stable adhesion of undeveloped and developed cells. a**, Force-spectroscopy traces for adhesions of growth-phase cells. Cell–cell contacts were maintained for 0.2 s at 90±10 pN. **b**, Histogram of de-adhesion forces for 960 traces under the same conditions as in **a**. Note that, despite the enhanced contact force (90 pN), only a small percentage of contacts resulted in measurable cell–cell adhesion. **c**, **d**, Force-spectroscopy traces for adhesions of *D. discoideum* cells at the developed stage after 6 h of starvation. Cell–cell contacts were maintained for 2 s (**c**) or 0.2 s (**d**) at 35±5 pN. Arrows in **c** indicate force steps for complete rupture as shown in histograms. **e**, Histogram of de-adhesion forces for 1,792 traces under the same conditions as in **c**. **f**, Histogram of de-adhesion forces for 1,088 traces. Cell–cell contacts were maintained for 1 s at 35±5 pN . **g**, Histogram of de-adhesion forces for 1,334 traces under the same conditions as in **d**. All curves were recorded in the presence of 5 mM EDTA. Data-point resolutions of 32,768 (**a**) or 256 (**c, d**) points per trace were used. In histograms, rupture events occurring at <7 pN are represented by the first bar.

ance, we picked up a *D. discoideum* cell with a tipless AFM cantilever, the end of which had been covalently functionalized with a lectin, resulting in firm attachment of the cell to the cantilever. A target cell at the bottom of a Petri dish was positioned underneath the cantilever-mounted cell, and was approached until a predefined repulsive contact force was established (Fig. 1). This contact force was held constant for a predefined time interval to allow establishment of cell adhesion. Upon retraction of the cantilever, we recorded the force as a function of the distance that the cantilever was moved until contact between the cells was broken.

A force trace for de-adhesion of two cells is shown in Fig. 2a (Ca^{2+} trace). This trace is typical of growth-phase cells that had been allowed to interact for 20 s at a contact force of 150 pN. The adhesion between these cells gave rise to unbinding forces of the order of 1 nN, caused by a multitude of molecular interactions that were not resolved under these conditions. Adhesion of the undeveloped cells used in this experiment is known to be Ca^{2+}-dependent[34]. To determine whether the measurement of de-adhesion forces reflects this Ca^{2+} sensitivity, we added a chelating agent, EDTA (see Methods), to the buffer; adhesion was drastically reduced (Fig. 2a, EDTA trace). At the concentration used, EDTA did not affect the integrity of cells during the experiment, as verified by monitoring cell shape and locomotion.

Controlled establishment of discrete interactions between live cells. Two steps of refinement of the technique were crucial for measuring discrete de-adhesion forces at molecular resolution — first, reduction of the contact force, leading to a decrease in contact area, and second, shortening of the contact time, to reduce the number of contacts established (Fig. 2b). After growth-phase cells were brought together by contact forces of 30–40 pN applied for

Table 1 Percentages of cells showing measurable adhesion forces in the presence of 5 mM EDTA.

Cell strain	Growth-phase cells	Developed cells
Wild-type	4 (n=960)	86 (n=132)
csA-deletion (gene disruption)	Not determined	26 (n=67)
csA-deletion (shotgun)	8 (n=1,984)	32 (n=104)
csA (*csA* promoter)	16 (n=30)	79 (n=353)
csA (*actin 15* promoter)	82 (n=149)	78 (n=256)

De-adhesion experiments were carried out as in Fig. 3b, g, except that contact forces were increased to 90±10 pN.
'Growth-phase' cells are undeveloped cells, in which the *actin 15* promoter is switched on but the *csA* promoter is not. 'Developed' cells are starved cells at the aggregation stage, in which the *csA* promoter has been switched on. For controlled expression of *csA*, the following strains were used: wild-type, AX2-214; *csA*-deletion strain generated by gene disruption, mutant T10 (ref. 35); *csA*-deletion generated by shotgun mutagenesis, HG1287 (ref. 36); strain expressing *csA* under the control of its own promoter, transformant CPH of HG1287 (ref. 36); strain expressing *csA* under the control of the *actin 15* promoter, transformant HTC1 of HG1287 (ref. 13).

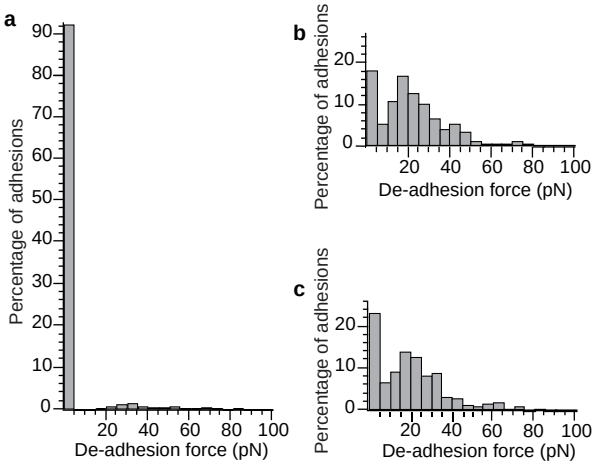

Figure 4 **De-adhesion forces for lipid-anchored csA and a transmembrane chimaera.** Histograms showing de-adhesion forces on the basis of force-spectroscopy traces using the cell strains indicated below. Measurements were obtained from growth-phase cells in the presence of 5 mM EDTA. **a**, HG1287, a *csA*-deletion strain in which 92% of cells showed no adhesion. Data were obtained from 1,984 traces. **b**, HTC1, a *csA*-deletion strain transfected with a vector encoding normal, phospholipid-anchored csA under the control of the *actin 15* promoter. Data were obtained from 149 traces. **c**, HTCP8 (ref. 13), a csA-deletion strain transfected with a vector encoding a chimaera, integrated into the membrane by a transmembrane polypeptide domain and controlled by the *actin 15* promoter. Note the presence of a well pronounced de-adhesion peak at 23 pN, as in **b**. Data were obtained from 544 traces.

only 0.2 s, <20% of de-adhesion traces showed binding between the cells. The histogram of de-adhesion forces (Fig. 2c) shows a broad distribution, with a maximum at 40–60 pN. On the basis of Poisson statistics, the low frequency of these de-adhesion events indicates that >90% of the contacts may represent single binding events. Thus, the width of the force distribution probably reflects the involvement of several molecular species in Ca^{2+}-dependent adhesion.

In the presence of EDTA, 96% of growth-phase cells did not establish detectable adhesions within 0.2 s, even when brought into contact with an increased force of 90 pN (Fig. 3a, b). We therefore measured de-adhesion forces in developing cells, in which further cell-adhesion proteins are expressed. Cells at the aggregation stage are distinguished from growth-phase cells by EDTA-stable cell adhesions[10]. When EDTA was added to these cells and de-adhesion forces were determined after a contact force of 35±5 pN, binding was observed in roughly 50% of traces. Figure 3c shows results obtained using a contact time of 2 s. We frequently found that initial forces rose up to several hundred pN and unbinding occurred in several steps, until the last tether connecting the two cells was disrupted. In contrast to these multiple de-adhesion events, de-adhesions after a contact time of 0.2 s predominantly involved a single step (Fig. 3d).

The last force step, after which cells were completely separated, was measured in more than 1,000 traces after contact times of 2 s, 1 s or 0.2 s. When these data were compiled in histograms, a pronounced peak indicating a force quantum of 23±8 (s.d.) pN became apparent (Fig. 3e–g). Upon reduction of contact times from 2 s to 0.2 s, this peak shifted only negligibly to lower de-adhesion forces. The main difference between the histograms for different force times is that larger rupture forces are not as evident at shorter contact times (Fig. 3e–g). We therefore interpret the larger forces contributing to de-adhesion after 2 s or 1 s of cell–cell contact as superimposed multiples of the basic force quantum of 23 pN.

Genetic manipulation links the 23 pN peak to csA expression. Developmental regulation and EDTA resistance indicate that the measured force quantum of 23 pN may be due to unbinding of csA molecules. However, cells at the aggregation stage differ from growth-phase cells not only in the expression of csA, but also in that of several other developmentally regulated cell-surface proteins. Therefore, in order to attribute the peak of 23 pN to the presence of csA in particular, we used three types of cells in which csA expression was genetically manipulated. First, the *csA* gene was selectively inactivated by targeted disruption, using a transformation vector that recombined into the gene's coding region[35]. Only 26% of cells of this *csA*-deletion strain showed measurable de-adhesion forces, as compared to 86% of wild-type cells (Table 1).

Second and third, cells of a mutant unable to produce csA[36], which was obtained by shotgun mutagenesis, were transfected with vectors encoding csA under the control of two different promoters. When controlled by its own developmentally regulated promoter, csA is absent during growth and is expressed during development. However, when controlled by the constitutively active *actin 15* promoter[37], csA is expressed in growing cells that normally lack this protein. When csA was expressed under the control of its own promoter, growth-phase cells showed no change, but the majority of developed cells showed adhesion (Table 1). When csA was expressed under the control of the *actin 15* promoter, however, adhesion was already detectable in 82% of growth-phase cells, as compared to 8% of control cells (Table 1). Together, these results demonstrate that csA is the principal source of the intercellular adhesion measured by force spectroscopy in the presence of EDTA.

Replacement of the phospholipid anchor does not affect de-adhesion forces. The findings described above can be interpreted to reflect de-adhesion in the strict sense, that is, dissociation of adhesion molecules from each other at an unbinding force of 23 pN. Alternatively, de-adhesion may be caused by extraction of the phospholipid anchor of the csA molecule from the plasma membrane[38]. To determine whether replacement of the lipid anchor affects de-adhesion forces, we used a *csA*-deletion strain (Fig. 4a) complemented with a chimaeric protein in which the phospholipid anchor of csA was replaced with a carboxy-terminal fragment of another protein, consisting of a hydrophobic transmembrane domain and a charged cytoplasmic domain. The transmembrane domain of this protein consists of 23 primarily hydrophobic amino-acid residues and the cytoplasmic tail comprises 34 residues, including 6 positively charged lysine or arginine residues and 3 negatively charged aspartate or glutamate residues[13]. The positively charged residues of the tail are thought to stabilize membrane integration by interacting with negatively charged lipid head groups at the cytoplasmic phase of the plasma membrane. This replacement of the csA anchor did not significantly alter de-adhesion forces, as shown by Fig. 4c in

comparison to Fig. 4b. These results support the idea that, upon forced separation of cells, the observed de-adhesion forces reflect molecular interactions that are independent of the way in which the cell-adhesion protein is attached to the membrane.

Discussion

We have resolved the de-adhesion forces for two types of cell interaction in *D. discoideum*—the Ca^{2+}-dependent cell–cell adhesion of undeveloped cells and the EDTA-resistant adhesion typical of aggregating cells. Although, at the nanonewton level, both types of adhesion resulted in massive adhesion with a more or less continuous de-adhesion process upon separation, discrete interactions were found in both cases at the piconewton level. At this level, Ca^{2+}-dependent adhesion is characterized by a comparably broad distribution of de-adhesion forces, which indicates that several molecular species with different adhesion characteristics may be involved in contact formation. In contrast, EDTA-stable cell adhesion peaked at 23 pN, indicating that a single molecular species may be responsible for most of these interactions. Previous studies have shown that this type of adhesion is primarily due to one particular cell-adhesion molecule, the csA glycoprotein[36,37].

Expression of the *csA* gene is controlled by a promoter that is inactive during cell growth and is switched on during early development immediately before the aggregation stage[36].Using three genetically manipulated strains, we have confirmed that csA is responsible for the majority of adhesion events detected in EDTA-treated cells at the aggregation stage (Table 1). Specific deletion of the *csA* gene, by homologous recombination, markedly reduced the probability of adhesion after short periods of cell–cell attachment from about 80% in wild-type cells to <30% in mutant cells. Overexpression of transfected *csA*, under the control of its own promoter, in csA-null mutant cells restored high adhesion efficiency, but this occurred only after the promoter was triggered by a period of development. As the vector encoded only csA (as well as the phosphotransferase marker used to select G418-resistant transformants), this recovery of adhesiveness is unequivocally attributable to csA. When *csA* was ectopically expressed in csA-null cells, under the control of the constitutively active *actin 15* promoter, a de-adhesion peak was observed at 23 pN in the growth phase (Fig. 4b), during which the *csA* gene is normally switched off (Table 1). These results demonstrate that it is sufficient to supplement the surfaces of growth-phase cells with vector-encoded csA in order to confer an adhesiveness that is typical of cells at the aggregation stage.

The quantified de-adhesion force of 23 pN indicates that the units of csA-mediated cell adhesion may be discrete molecular entities. The most obvious interpretation of this peak is that one unit reflects the interaction of two csA molecules, one on each cell surface. Nevertheless, as oligomerization may increase the affinity of cell-adhesion molecules for one another[39], we cannot exclude the possibility that defined dimers or oligomers represent the functional units of csA interactions.

As the bond-rupture experiments were carried out under non-equilibrium conditions, the observed forces are rate-dependent. As shown previously[32,33,40], this rate-dependence may provide further information regarding binding potential. For living cells, this detailed analysis will be important to link cell adhesion to the rate of cell movement or to shear forces in the bloodstream[17]. Here we kept the separation rate constant at 2.5 $\mu m\,s^{-1}$, resulting in force ramps of 100–500 $pN\,s^{-1}$ depending on cellular elasticity. This rate is of the same order of magnitude as the retraction rates of filopods, the fastest cell-surface extensions in *D. discoideum* cells. As they have adhesive ends, filopods can form contacts between cells or between cells and other surfaces. Our measurements of separation forces therefore represent the upper limits to which the cells are exposed by their own motility.

We considered the possibility that the de-adhesion forces measured reflect extraction of the lipid anchor from the membrane, rather than dissociation of the interacting protein moieties of the csA molecules[41]. To alter insertion of the protein into the membrane, the lipid anchor was replaced with the carboxy-terminal fragment of another protein, consisting of a transmembrane domain and a cytoplasmic tail. The same peak de-adhesion value of 23 pN was observed for this chimaeric transmembrane protein as for the normal, lipid-anchored csA molecule (Fig. 4).

On the basis of changes in free energy that are associated with the displacement of charged residues into a lipid layer and of hydrophobic residues into an aqueous environment, it has been calculated[42] that about 100 pN is required to uproot glycophorin, a transmembrane protein present in the membranes of erythrocytes. This estimate is in accordance with the anchoring forces of 80–170 pN recently observed for the α-helices of bacteriorhodopsin in the purple membrane[20]. As the amino-acid sequence of our chimaeric construct indicates that it is at least as tightly integrated into the plasma membrane as glycophorin, it seems unlikely that the peak of 23 pN reflects uprooting of the protein from the membrane. Although we cannot exclude the possibility that the largest forces observed reflect such protein extraction, we propose that the force peak measured upon separation of cells represents detachment of csA binding sites from one another. The possibility that the observed forces reflect ruptures between cells can be ruled out for the vast majority of traces because of the continuously increasing positive slopes of force ramps, which contrast with the slopes of almost zero that characterize tether extension.

The measured de-adhesion force of 23 pN for csA is small in comparison with those for most antibody–antigen or lectin–sugar interactions, which frequently exceed 50 pN at comparable rupture rates[43]. The moderate intermolecular forces involved in cell-adhesion are consistent with the ability of motile cells to glide against each other as they become integrated into a multicellular structure. Moreover, in view of the limited force that the lipid anchor can withstand, much higher molecular-unbinding forces would confer no advantage. As shown by the interaction of lipid vesicles supplemented with csA, membrane adhesion can be strengthened by lateral diffusion of adhesion proteins[44].

We have combined nanophysics with cell biology to establish a mechanical assay that quantitatively links the expression of a gene to the function of its product in cell adhesion. This type of single-molecule force spectroscopy using live cells is directly applicable to a variety of different cell-adhesion systems. This assay has a wide field of potential applications, such as in the investigation of mutated cell-adhesion proteins or of coupling of cell-adhesion molecules to the cytoskeleton, and also in the evaluation of adhesion-blocking drugs. Furthermore, this technique could be used to investigate the initial steps in the interaction of cells with natural and artificial surfaces of medical interest, such as the receptor-mediated adhesion of particles to phagocyte surfaces. □

Methods

D. discoideum cell culture.

All mutants were derived from the *D. discoideum* AX2-214 strain, designated here as the wild type. Mutant HG1287 was generated by E. Wallraff as described[36]. In this mutant, *csA* expression was eliminated by a combination of chemical and ultraviolet-induced mutagenesis. Because of this 'shotgun' mutagenesis, other genes besides *csA* may also have been inactivated. Cells were cultivated in Petri dishes in nutrient medium[45], to a density of 1×10^6 cells ml^{-1}. For transformants HTC1 and HTCP8 (ref. 13), CPH[37] and T10 (ref. 35), 20 $\mu g\,ml^{-1}$ of the selection marker G418 was added to stabilize *csA* expression. Before measurements were taken, cells were washed and resuspended in 17 mM K/Na buffer, pH 6.0, and used either immediately as undeveloped cells, or as developed cells after shaking for about 6 h at 150 r.p.m. Experiments were carried out at about 20 °C.

Cantilever preparation.

The softest triangular shaped microlevers (Parc Scientific Instruments, Sunnyvale, California) with a spring constant of $4.8\pm0.5\,mN\,m^{-1}$ (calibrated using the thermal noise amplitude[46,47]) were used. The pyramidal tip was chipped away to obtain a plane surface for cell contact. The lever was then washed in ethanol, silanized in N′-(3-(trimethoxysilyl)-propyl)-diethylentriamin (Aldrich, Milwaukee, Wisconsin) and rinsed in ethanol and water. After incubation in PBS, pH 7.4 (Sigma), containing 10 $mg\,ml^{-1}$ 1-ethyl-3-(3-dimethylaminopropyl)carbodiimide (Sigma), 10 $mg\,ml^{-1}$ N-hydroxysuccinimide (Aldrich) and 10 $mg\,ml^{-1}$ carboxyamylose for 10 min, the lever was rinsed three times in PBS and then coated with 50 $\mu g\,ml^{-1}$ wheatgerm agglutinin (WGA; Sigma) in PBS for at least 1 h; it was then rinsed and stored in pure PBS.

Instrumental setup.

Experiments were carried out with a home-built force spectrometer as described[43]. An AFM cantilever was positioned using a piezoelectric crystal, with a range of 8 µm or 80 µm, and a strain-gage position sensor; its deflection was measured by laser reflection onto a split photodiode. Positioning precision in the z-direction was 1 Å, and force sensitivity was within 3 pN. Unless stated otherwise, the cantilever was moved with a velocity of $2.5 \pm 0.5\,\mu m\,s^{-1}$. Data were oversampled 30-fold with a data-point frequency of 60 kHz, at a resolution of 256 or 32,768 data points.

Force spectroscopy.

Cells suspended in 17 mM K/Na-phosphate buffer, pH 6.0, were spread on polystyrene Petri dishes of 3.5-cm diameter, at a density of about 100 cells mm^{-2}. To chelate Ca^{2+}, 5 mM EDTA was added at pH 6.0 to the same buffer. To avoid scattering of the laser beam of the detection system, non-adherent cells were removed by gently rinsing the dish after 10 min. An attached cell was slightly loosened by pushing its flank with the side of the cantilever. The extreme end of the lever was then lowered onto the cell at a force of a few nN and held in contact for approximately 30 s to allow the lectin on the lever to bind; the cell was then lifted off the bottom of the dish. Another cell was approached with the cantilever-mounted cell and the interaction was measured as described above. As target cells tended to move on the surface of the dish, it was necessary to check the cell contact using the built-in light microscope and readjust the positioning of cells. Peak values ± s.d. were derived from histograms by Gaussian fits, calculated using the standard algorithm of IgorPro 3.11.

RECEIVED 8 DECEMBER 1999; REVISED 30 MARCH 2000; ACCEPTED 31 MARCH 2000; PUBLISHED 28 APRIL 2000.

1. Vestweber, D. & Blanks, J. E. Mechanisms that regulate the function of the selectins and their ligands. *Physiol. Rev.* **79,** 181–213 (1999).
2. Fritz, J., Katopodis, A. G., Kolbinger, F. & Anselmetti, D. Force-mediated kinetics of single P-selectin/ligand complexes observed by atomic force microscopy. *Proc. Natl Acad. Sci. USA* **95,** 12283–12288 (1998).
3. Springer, T. A. Adhesion receptors of the immune system. *Nature* **346,** 425–434 (1990).
4. Kreis, T. & Vale, R. (eds) *Guidebook to the Extracellular Matrix, Anchor, and Adhesion Proteins* (Oxford Univ. Press, 1999).
5. Faix, J. in *Guidebook to the Extracellular Matrix, Anchor, and Adhesion Proteins* (eds Kreis, T. & Vale, R.) 177–179 (Oxford Univ. Press, 1999).
6. Ponte, E., Bracco, E., Faix, J. & Bozzaro, S. Detection of subtle phenotypes: the case of the cell adhesion molecule csA in *Dictyostelium*. *Proc. Natl Acad. Sci. USA* **95,** 9360–9365 (1998).
7. Bozzaro, S. & Gerisch, G. Contact sites in aggregating cells of *Polysphondylium pallidum*. *J. Mol. Biol.* **120,** 265–279 (1978).
8. Gerisch, G., Krelle, H., Bozzarro, S., Eitle, E. & Guggenheim, R. in *Cell Adhesion and Motility* (eds Curtis, A. S. G. & Pitts, J. D.) 293–307 (Cambridge Univ. Press, Cambridge, UK, 1980).
9. Murray, B. A., Yee, L. D. & Loomis, W. F. Immunological analysis of glycoprotein (contact sites A) involved in intercellular adhesion of *Dictyostelium discoideum*. *J. Supramol. Struct. Cell. Biochem.* **17,** 197–211 (1981).
10. Beug, H., Katz, F. E. & Gerisch, G. Dynamics of antigenic membrane sites relating to cell aggregation in *Dictyostelium discoideum*. *J. Cell Biol.* **56,** 647–658 (1973).
11. Siu, C.H. *et al.* Molecular mechanisms of cell–cell interaction in *Dictyostelium discoideum*. *Biochem. Cell Biol.* **66,** 1089–1099 (1988).
12. Stadler, J., Keenan, T. W., Bauer, G. & Gerisch, G. The contact site A glycoprotein of *Dictyostelium discoideum* carries a phospholipid anchor of a novel type. *EMBO J.* **8,** 371–377 (1989).
13. Barth, A., Müller-Taubenberger, A., Taranto, P. & Gerisch, G. Replacement of the phospholipid-anchor in the contact site A glycoprotein of *Dictyostelium discoideum* by a transmembrane region does not impede cell adhesion but reduces residence time on the cell surface. *J. Cell Biol.* **124,** 205–215 (1994).
14. Evans, E. A. Detailed mechanics of membrane–membrane adhesion and separation II. Discrete kinetically trapped molecular cross-bridges. *Biophys. J.* **48,** 185–192 (1985).
15. Evans, E. in *Structure and Dynamics of Membranes* (eds Lipowsky, R. & Sackmann, E.) 723–754 (Elsevier, Amsterdam, 1995).
16. Curtis, A. S. G. Problems and some solutions in the study of cellular aggregation. *Symp. Zool. Soc. Lond.* **25,** 335–352 (1970).
17. Chen, S. & Springer, T. A. An automatic braking system that stabilizes leukocyte rolling by an increase in selectin bond number with shear. *J. Cell Biol.* **144,** 185–200 (1999).
18. Binnig, G., Quate, C. F. & Gerber, C. Atomic force microscope. *Phys. Rev. Lett.* **56,** 930–933 (1986).
19. Gimzewski, J. K. & Joachim, C. Nanoscale science of single molecules using local probes. *Science* **283,** 1683–1688 (1999).
20. Oesterhelt, F. *et al.* Unfolding pathways of individual bacteriorhodopsins. *Science* (in the press).
21. Rief, M., Oesterhelt, F., Heymann, B. & Gaub, H. E. Single molecule force spectroscopy on polysaccharides by AFM. *Science* **275,** 1295–1297 (1997).
22. Marszalek, P. E. *et al.* Atomic levers control pyranose ring conformations. *Proc. Natl Acad. Sci. USA* **96,** 7894–7898 (1999).
23. Rief, M., Gautel, M., Schemmel, A. & Gaub, H. E. The mechanical stability of immunoglobulin and fibronectin III domains in the muscle protein titin measured by AFM. *Biophys. J.* **75,** 3008–3014 (1998).
24. Oberhauser, A. F., Marszalek, P. E., Erickson, H. P. & Fernandez, J. M. The molecular elasticity of the extracellular matrix protein tenascin. *Nature* **393,** 181–185 (1998).
25. Smith, B. L. *et al.* Molecular mechanistic origin of the toughness of natural adhesives, fibres and composites. *Nature* **399,** 761–763 (1999).
26. Rief, M., Clausen-Schaumann, H. & Gaub, H. E. Sequence-dependent mechanics of single DNA molecules. *Nature Struct. Biol.* **6,** 346–349 (1999).
27. Strunz, T., Oroszlan, K., Schäfer, R. & Güntherodt, H-J. Dynamic force spectroscopy of single DNA molecules. *Proc. Natl Acad. Sci. USA* **96,** 11277–11282 (1999).
28. Moy, V. T., Florin, E-L. & Gaub, H. E. Intermolecular forces and energies between ligands and receptors. *Science* **266,** 257–259 (1994).
29. Florin, E-L., Moy, V. T. & Gaub, H. E. Adhesive forces between individual ligand-receptor pairs. *Science* **264,** 415–417 (1994).
30. Hinterdorfer, P., Baumgartner, W., Gruber, H. J., Schilcher, K. & Schindler, H. Detection and localization of individual antibody-antigen recognition events by atomic force microscopy. *Proc. Natl Acad. Sci. USA* **93,** 3477–3481 (1996).
31. Müller, K. M., Arndt, K. M. & Plückthun, A. Model and simulation of multivalent binding to fixed ligands. *Anal. Biochem.* **261,** 149–158 (1998).
32. Grubmüller, H., Heymann, B. & Tavan, P. Ligand binding: molecular mechanics calculation of the streptavidin–biotin rupture force. *Science* **271,** 997–999 (1996).
33. Merkel, R., Nassoy, P., Leung, A., Ritchie, K. & Evans, E. Energy landscapes of receptor–ligand bonds explored with dynamic force spectroscopy. *Nature* **397,** 50–53 (1999).
34. Beug, H., Katz, F. E., Stein, A. & Gerisch, G. Quantitation of membrane sites in aggregating *Dictyostelium* cells by use of tritiated univalent antibody. *Proc. Natl Acad. Sci. USA* **70,** 3150–3154 (1973).
35. Harloff, C., Gerisch, G. & Noegel, A. A. Selective elimination of the contact site A protein of *Dictyostelium discoideum* by gene disruption. *Genes Dev.* **3,** 2011–2019 (1989).
36. Faix, J., Gerisch, G. & Noegel, A. A. Overexpression of the csA cell adhesion molecule under its own cAMP-regulated promoter impairs morphogenesis in *Dictyostelium*. *J. Cell Sci.* **102,** 203–214 (1992).
37. Faix, J., Gerisch, G. & Noegel, A. A. Constitutive overexpression of the contact site A glycoprotein enables growth-phase cells of *Dictyostelium discoideum* to aggregate. *EMBO J.* **9,** 2709–2716 (1990).
38. Evans, E. Energy landscapes of biomolecular adhesion and receptor anchoring at interfaces explored with dynamic force spectroscopy. *R. Soc. Chem: Faraday Discuss.* **111,** 1–16 (1998).
39. Tomschy, A., Fauser, C., Landwehr, R. & Engel, J. Homophilic adhesion of E-cadherin occurs by a co-operative two-step interaction of N-terminal domains. *EMBO J.* **15,** 3507–3514 (1996).
40. Rief, M., Fernandez, J. M. & Gaub, H. E. Elastically coupled two-level systems as a model for biopolymer extensibility. *Phys. Rev. Lett.* **81,** 4764–4767 (1998).
41. Evans, E., Berk, D. & Leung, A. Detachment of agglutinin bonded red blood cells I. Forces to rupture molecular point attachments. *Biophys. J.* **59,** 838–848 (1991).
42. Bell, G. I. Models for the specific adhesion of cells to cells. *Science* **200,** 618–627 (1978).
43. Dettmann, W. *et al.* Differences in zero-force and force-driven kinetics of ligand dissociation from β-galactoside-specific proteins (plant and animal lectins, immunoglobulin G) monitored by plasmon resonance and dynamic single molecule force microscopy. *Arch. Biochem. Biophys.* (in the press).
44. Kloboucek, A., Behrisch, A., Faix, J. & Sackmann, E. Adhesion-induced receptor segregation and adhesion plaque formation: a model membrane study. *Biophys. J.* **77,** 2311–2328 (1999).
45. Malchow, D., Nägele, B., Schwarz, H. & Gerisch, G. Membrane-bound cyclic AMP phosphodiesterase in chemotactically responding cells of *Dictyostelium discoideum*. *Eur. J. Biochem.* **28,** 136–142 (1972).
46. Florin, E. L. *et al.* Sensing specific molecular interactions with the atomic force microscope. *Biosensors Bioelectr.* **10,** 895–901 (1995).
47. Butt, H. J. & Jaschke, M. Thermal noise in atomic force microscopy. *Nanotechnol.* **6,** 1–7 (1995).

ACKNOWLEDGEMENTS

We thank M. Westphal and E. Simmeth for culturing *Dictyostelium*, and W. Dettmann for instrumentation and discussions. This work was supported by grants from the VW Foundation and the Deutsche Forschungsgemeinschaft..

Correspondence and requests for materials should be addressed to M.B.

